

UC Davis

UC Davis Previously Published Works

Title

G2/M arrest and mitotic slippage induced by fenbendazole in canine melanoma cells

Permalink

<https://escholarship.org/uc/item/40h0r9xh>

Journal

Veterinary Medicine and Science, 8(3)

ISSN

2053-1095

Authors

Kim, Sehoon
Perera, Shashini Kanchanamala
Choi, Seo-In
et al.

Publication Date



2022-05-01

DOI

10.1002/vms3.733

Peer reviewed

G2/M arrest and mitotic slippage induced by fenbendazole in canine melanoma cells

Sehoon Kim¹  | Shashini Kanchanamala Perera¹ | Seo-In Choi¹ |
Robert B. Rebhun²  | Kyoung-won Seo³

¹ Department of Veterinary Internal Medicine, College of Veterinary Medicine, Chungnam National University, Daejeon, Korea

² Center for Companion Animal Health, Department of Surgical and Radiological Sciences, School of Veterinary Medicine, University of California, Davis, California

³ Department of Veterinary Internal Medicine, College of Veterinary Medicine, Seoul National University, Korea, Seoul

Correspondence

Kyoung-won Seo, Department of Veterinary Internal Medicine, College of Veterinary Medicine, Seoul National University, Seoul, Korea.

Email: kwseo@snu.ac.kr

Funding information

Rural Development Administration, Republic of Korea, Grant/Award Number: PJ01404502

Abstract

Background: The use of fenbendazole (FBZ) in terminal cancer patients has recently increased, as anthelmintic drugs, such as FBZ and benzimidazole, exhibit anti-tubulin effects in tumour cells.

Objectives: The present study evaluated the in vitro anti-cancer effects of FBZ in five canine melanoma cell lines originating from the oral cavity (UCDK9M3, UCDK9M4, UCDK9M5, KMeC and LMeC).

Methods: Five canine melanoma cell lines were treated with FBZ and analysed with cell viability assay, cell cycle analysis, western blot assay and immunofluorescence staining to identify apoptotic effect, cell cycle arrest, microtubule disruption and mitotic slippage.

Results: Cell viability was reduced in all melanoma cell lines in a dose-dependent manner after FBZ treatment. Through cell cycle analysis, G2/M arrest and mitotic slippage were identified, which showed a time-dependent change. All treatment concentrations induced increased cleaved PARP signals in western blot analysis compared to the control groups. Immunofluorescence of cells treated for 24 h revealed defects in microtubule structure, multinucleation or macronucleation. With the exception of UCDK9M3, the melanoma cells showed mitotic slippage and post-slippage death, indicative of mitotic catastrophe.

Conclusions: These results indicate that FBZ exhibits anti-cancer effects in vitro against canine melanoma cells; however, further in vivo studies regarding the clinical applications of FBZ are required.

KEYWORDS

anti-tumour effect, apoptosis, canine melanoma cell, fenbendazole, G2/M cell cycle arrest, mitotic slippage

This is an open access article under the terms of the [Creative Commons Attribution-NonCommercial-NoDerivs](https://creativecommons.org/licenses/by-nc-nd/4.0/) License, which permits use and distribution in any medium, provided the original work is properly cited, the use is non-commercial and no modifications or adaptations are made.

© 2022 The Authors. *Veterinary Medicine and Science* published by John Wiley & Sons Ltd.

1 | INTRODUCTION

Malignant melanoma is a relatively common neoplasia in dogs (Inoue et al., 2004; Vail, 2020). Oral melanoma is the most commonly diagnosed malignant cancer arising in the oral cavity in dogs (Bolon et al., 1990; Obradovich, 2016; Vail, 2020). Melanomas originating in the oral cavity exhibit highly variable behaviour based on their anatomical site, size, stage and histological parameters. Higher grade and larger size oral melanomas carry a poor-to-grave prognosis (Obradovich, 2016; Vail, 2020). Local control can be achieved in some cases with surgical excision, xenogenic DNA vaccine and/or radiation therapy, but in advanced cases treatment options are limited (Rogers, 2000).

Fenbendazole (FBZ) is a benzimidazole drug that is used as an anthelmintic to treat various parasitic diseases in animals. It is generally regarded as safe with minimal side effects in dogs compared to the other anthelmintic drugs (Dogra et al., 2018). Some benzimidazole drugs, including FBZ, bind to the colchicine binding site (Koch, 2017; Schmit, 2013) and exhibit anti-cancer effects by inhibiting tubulin polymerisation (Dogra et al., 2018; Doudican et al., 2008; Lai et al., 2017; Pinto et al., 2019; Sasaki et al., 2002). In addition, a study in human melanoma cells indicated that FBZ also exhibits anti-cancer effects by modulating several cellular pathways (Dogra et al., 2018).

Microtubule-targeting agents (MTAs) disrupt the cell cycle and induce mitotic arrest in rapidly dividing tumour cells, which can result in cancer cell apoptosis (Stanton et al., 2011). Cancer cells reportedly display a sensitivity to mitotic defects, which represents a major target for anti-cancer chemotherapy (Mc Gee, 2015). MTAs can be classified into microtubule-stabilising and microtubule-destabilising agents (Li et al., 2018; Stanton et al., 2011). Microtubule-destabilising agents disrupt microtubule dynamics and lead to apoptosis in dividing cells (Stanton et al., 2011). In addition, MTAs have apoptotic effects during prolonged mitotic arrest (Shi et al., 2011) and induce p53-dependent post-slippage apoptosis (Zhu et al., 2014).

Mitotic catastrophe is defined by the International Nomenclature Committee on Cell Death as a regulated oncosuppressive mechanism for the control of mitosis-incompetent cells by regulated cell death or cellular senescence (Blagosklonny, 2007; Portugal et al., 2009; Vitale et al., 2011). Morphologically, mitotic catastrophe is defined by unique nuclear changes that include enlarged cells with multiple multinucleation, micronucleation or macronucleation (Castedo et al., 2004; Singh et al., 2012). It potentially occurs as a consequence of chromosomal mis-segregation or from the persistence of lagging or acentric chromosomes, although the precise molecular mechanisms of the mitotic catastrophe cascade are not fully understood (Galluzzi et al., 2018). In the context of mitotic catastrophe, mitotic slippage describes a cell fate in which a cell does not die during mitotic arrest, escaping apoptosis, and instead exits mitosis without proper cell division, becoming a tetraploid cell (Blagosklonny, 2007).

Different studies have shown various FBZ effective doses in canine cancer cells, including canine glioma and canine osteosarcoma cells (Lai et al., 2017; Schmit, 2013). A study that looked at human non-small

cell lung carcinoma (A549 cell) showed strong reduction in cell viability (Dogra et al., 2018). The goal of the present study was to investigate the anti-cancer effects of FBZ, and specifically the influence of this drug on apoptosis and cell cycle disruption in canine melanoma cell lines.

2 | METHODS

2.1 | Cell culture and cell line validation statement

Five canine melanoma cell lines (UCDK9M3, UCDK9M4, UCDK9M5, KMeC and LMeC) originating from the oral cavity were chosen. UCDK9M3, UCDK9M4 and KMeC were generated from primary oral tumour and UCDK9M5 and LMeC were originated from lymph node metastasis from primary oral tumours (Aina et al., 2011; Pinto et al., 2019). UCDK9M3, UCDK9M4 and UCDK9M5 were kindly provided by Dr. Michael Kent and KMeC and LMeC were provided by Dr. Takayuki Nakagawa.

UCDK9M3, UCDK9M4, UCDK9M5 and KMeC were cultured in Dulbecco's modified Eagle's medium (DMEM; PAN Biotech, Aidenbach, Germany) supplemented with 10% FBS (VWR International, Radnor, Pennsylvania) and 1% antibiotic (penicillin and streptomycin) solution (Gibco BRL Ltd., Paisley, Scotland). LMeC cells were cultured in RPMI 1640 (HyClone, South Logan, Utah) with 10% FBS and 1% antibiotic (penicillin, streptomycin) solution. All cell lines were incubated at 37°C in a 5% CO₂ humidified incubator. FBZ was purchased from Sigma Aldrich (St. Louis, Missouri) and dissolved in dimethyl sulfoxide (DMSO; Sigma Aldrich) as a stock solution and diluted directly in culture medium. The highest DMSO concentration for cell viability assay was 0.3% at 100 µM FBZ and 0.15% at 50 µM for cell cycle and western blot analysis.

2.2 | Cell viability assay

Cell viability was assessed by 3-(4,5-dimethyl-2-yl)-5-(3-carboxymethoxyphenyl)-2-(4-sulfophenyl)-2H-tetrazolium (MTS) assay (Cell-Titer 96 Aqueous Non-radioactive Cell Proliferation Assay, Promega Inc, Wisconsin). A total of 3000 cells per well were seeded in a 96-well plate and incubated overnight, then treated with 100 µl of FBZ at various concentrations for 48 h. The treatment solution in each well was replaced by 100 µl of fresh medium, and 20 µl of MTS reagent was added to each well and incubated at 37°C for 2 h. Absorbance was measured with a microplate reader (ELx800, Biotek) at 490 nm. The viability was expressed using the following formula: % of control cells = [(Optical density (OD) of treated sample - OD of blanks)] / (OD of control sample - OD of blanks) × 100%. Each of the cell lines was assayed in triplicate, and the viability assay was repeated three times. Half maximal inhibitory concentration (IC₅₀) values were calculated using a four-parameter logistic curve with Graphpad Prism 8.4.0; accordingly the data were normalised and fitted (log(inhibitor) vs. normalised response with variable slope).

2.3 | Colony forming assay

The colony forming assay was performed by seeding 500 cells per well in 6-well plate and incubating for 8 h prior to treatment with various concentrations of FBZ for 12 h, washed with PBS and then incubated for 7–9 days depending on the confluence of the control wells. 0.05% crystal violet solution was used to stain colonies. All experiments were performed in triplicate.

2.4 | Cell cycle analysis with flow cytometry

A total of 5×10^5 cells of all five melanoma cell lines were plated in 6-well culture plates or in 60 mm dishes with complete medium and incubated overnight. One group of melanoma cells was treated with 0.2, 0.5, 1, 5 or 50 μM of FBZ for 24 h. Another group of melanoma cells was treated with 0.5, 1 or 5 μM , and was analysed every 8 h for 48 h. Cells remaining in the treated medium, as well as cells that may have washed out with PBS, were collected. Attached cells were also harvested with trypsin. Harvested cells were fixed with 70% cold ethanol, then incubated overnight at -20°C . Fixed cells were washed with PBS, then 2.5×10^5 cells were collected and stained with 0.5 ml of propidium iodide/RNase staining buffer (BD Transduction Laboratories, San Diego, California) to be analysed by flow cytometry using a BD Accuri C6 plus with BD Accuri 6 plus software. Cell cycle analysis was conducted within 1 h and each treatment was performed in triplicate for each cell line. The cell populations were identified by their distinctive position on forward and side-scatter plots. For each sample, at least 10,000 events within G0/1, S and G2/M phase were acquired to compare cell cycles depending on treatment dose or treatment time. An expanded gate was used to count sub-G1 and $>4\text{N}$ population. Total events for G0/1, S, G2/M phase, sub-G1 and $>4\text{N}$ are presented as percentages. The percentage of data is expressed as a stacked-bar graph and bar graph.

2.5 | Protein extraction and western blotting

One group of melanoma cells was treated with various concentrations of FBZ for 24 h. Another group of melanoma cells was treated with 0.5, 1 or 5 μM and analysed every 8 h for 48 h. Protein extraction was conducted using radioimmunoprecipitation assay lysis buffer (Santa Cruz Biotechnology, Inc., Santa Cruz, California) with protease inhibitor (Complete Protease Inhibitor Cocktail, Roche Diagnostics, Basel, Switzerland). After incubation on ice, cell lysates were centrifuged at 14,000 RPM (10,000 g), 4°C for 20 min and supernatants were collected. The standard curve obtained from a Bicinchoninic Acid assay was utilised to calculate protein concentration. Diluted samples with sample buffer (SmartGene 5X Sample buffer, SamJung Bioscience, Daejeon, Korea) were heated for 5 min at 100°C . Samples containing 10 μg protein were separated via SDS-polyacrylamide gel electrophoresis and transferred to nitrocellulose membranes. After blocking with 5% skim milk in TBST, membranes were probed

with primary antibodies. The primary antibodies were mouse monoclonal anti-cleaved PARP (1:1000 dilution; ABclone Technology, Massachusetts), mouse anti-GAPDH (1:10,000 dilution; ABclone) and mouse anti-cyclinB1 (1:250 dilution; BD Transduction Laboratories). Membranes were incubated with HRP-conjugated secondary antibodies (1:5000 dilution; Santa Cruz Biotechnology) for 1 h and the bound antibodies were visualised with chemiluminescent substrate (SmartGene ECL High Femto Solution, SamJung Bioscience) and a Las 4000 imager (GE Healthcare Biosciences, Uppsala, Sweden).

2.6 | Immunofluorescence assay

Melanoma cells were seeded in 35 mm dishes containing glass coverslips at a density of 5×10^5 for 8 h, then exposed to 0.5, 1 or 5 μM FBZ or media only as a control for 24 h. Cells were washed with PBS twice and fixed with 4% paraformaldehyde for 10 min at room temperature. 0.5% Triton X-100 (Samchun chemicals, Seoul, Korea) was used for permeabilisation for 10 min and cells were blocked with 1% bovine serum albumin (MP biomedical, Illkirch, France) for 30 min at room temperature. Cells were incubated in mouse monoclonal anti- α -tubulin antibody (1:500 dilution; ABclone) for 12 h at 4°C before incubating with goat anti-mouse IgG labelled with FITC (1:500 dilution; ABclone) for 1 h at room temperature. Cells were washed with PBS and coverslips were mounted with mounting solution with DAPI (Invitrogen, California). Cells were examined by confocal microscopy using a fluorescein filter (LSM 880 with Airyscan, Carl zeiss, Germany).

2.7 | Statistics

All analyses were performed using Graphpad Prism 8.4.0. software (GraphPad Software, Inc. San Diego, CA). The results from cell cycle analysis were compared using the Kruskal–Wallis test to calculate the significance, followed by Dunn's test. All values in this study are expressed as mean and standard deviation. A p value less than 0.05 was considered significant.

3 | RESULTS

3.1 | FBZ reduced cell viability of canine melanoma cell lines

A cell viability assay was performed to investigate the effects of FBZ on the survival of five canine melanoma cell lines. All cell lines showed reduced viability in a dose-dependent manner (Figure 1a). A significant decrease in the number of cancer cells was detected at 1 μM FBZ treatment. At 100 μM , the viability of all cell lines was decreased below 20%. The concentrations of FBZ that reduced the survival of each cell line by 50% (IC_{50} values) were 1.47 μM for UCDK9M3, 0.59 μM for UCDK9M4, 4.10 μM for UCDK9M5, 0.47 μM for KMeC and 1.98 μM for LMeC. A colony forming assay, used to determine cell survival as a

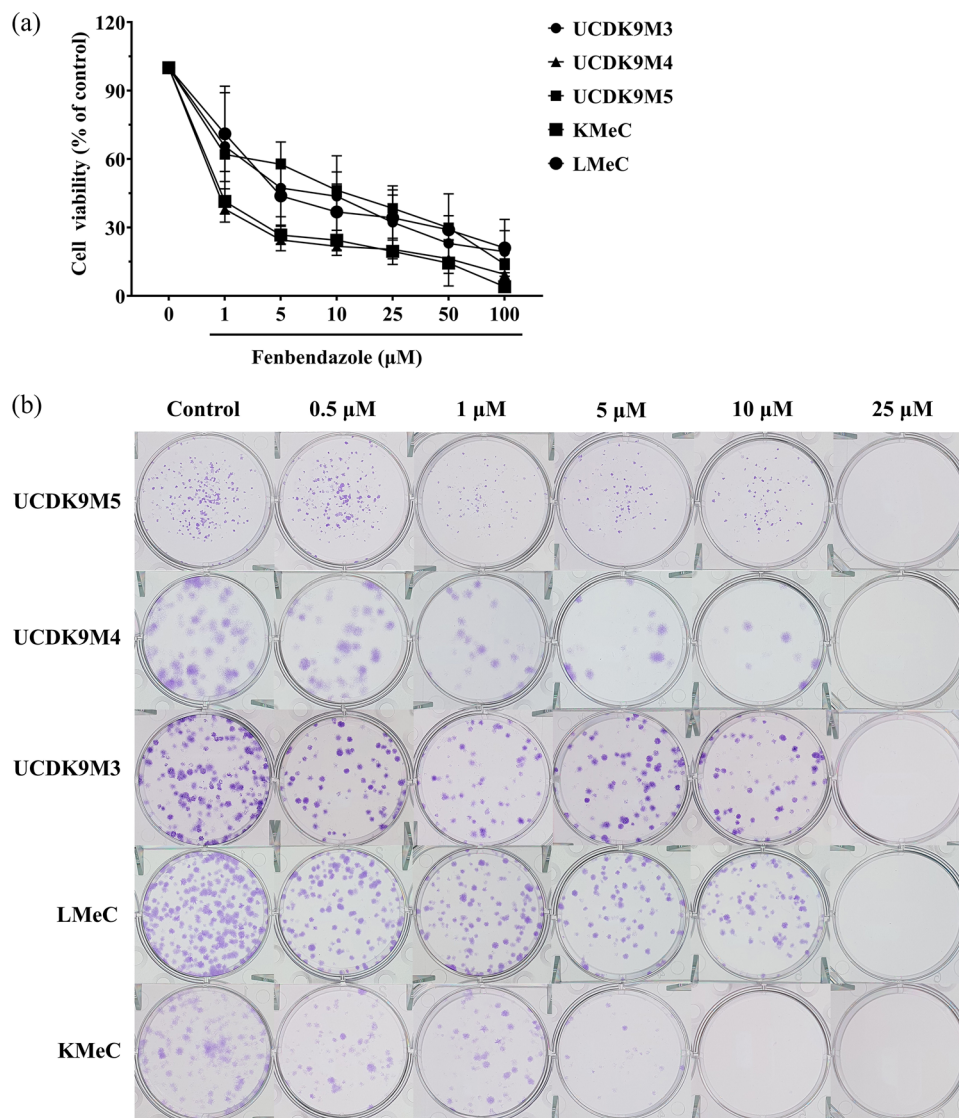


FIGURE 1 The effect of FBZ on the viability of canine melanoma cells. Melanoma cells were treated with different FBZ concentrations for 48 h (a). Colony forming assay for five canine melanoma cell lines (b). Each data point represents the mean \pm standard deviation

complementary method, showed growth inhibition. Exposure to 25 μ M FBZ for 12 h completely inhibited cell growth and reduced the colony formation further from 0.5 μ M FBZ treatment (Figure 1b).

3.2 | FBZ induces G2/M arrest

Twenty-four hours of exposure to FBZ resulted in increased numbers of cells in the G2/M phase for all cell lines (Figure 2a and b). At 0.2 μ M, none of the cell lines exhibited cell cycle phase shifts. While UCDK9M3 showed a drastic change in the G2/M phase at 0.5 μ M treatment, the other four cell lines exhibited the G2/M arrest at around 1 μ M. In addition, the G2/M ratio at 5 μ M was highest for UCDK9M5 (90.36 \pm 1.65; Figure 2b, Table 1). Gating of propidium iodide-height and propidium iodide-area (Figure 2c) revealed a cell cycle shift and arrest. With 0.5 or 1 μ M treatments, polyploid cells and changes in cell size were identified.

Cells treated and analysed at multiple time points showed an increase in S phase beginning at 8 h due to a cell cycle shift from G0/G1 to G2/M (Figure 2d, Table 2). After 8 h, the ratio of S phase was restored as the G2/M arrest occurred. At 0.5 and 1 μ M treatment, the G2/M arrest reached a peak at 8 or 16 h, except for UCDK9M3, which peaked at 40 h. At 5 μ M treatment, G2/M arrest was maximised or maintained.

3.3 | Sub-G1 in a dose-dependent manner and mitotic slippage

In cells treated with FBZ for 24 h, the sub-G1 population increased with increasing dose, but the peak concentration varied between cell lines (Figure 2e, Table 3). The sub-G1 population in UCDK9M3 cells increased at 0.2 μ M, but the >4N population of UCDK9M3 did not notably increase at any concentrations (Figure 2e). The other four cell lines showed remarkably increased sub-G1 populations at different

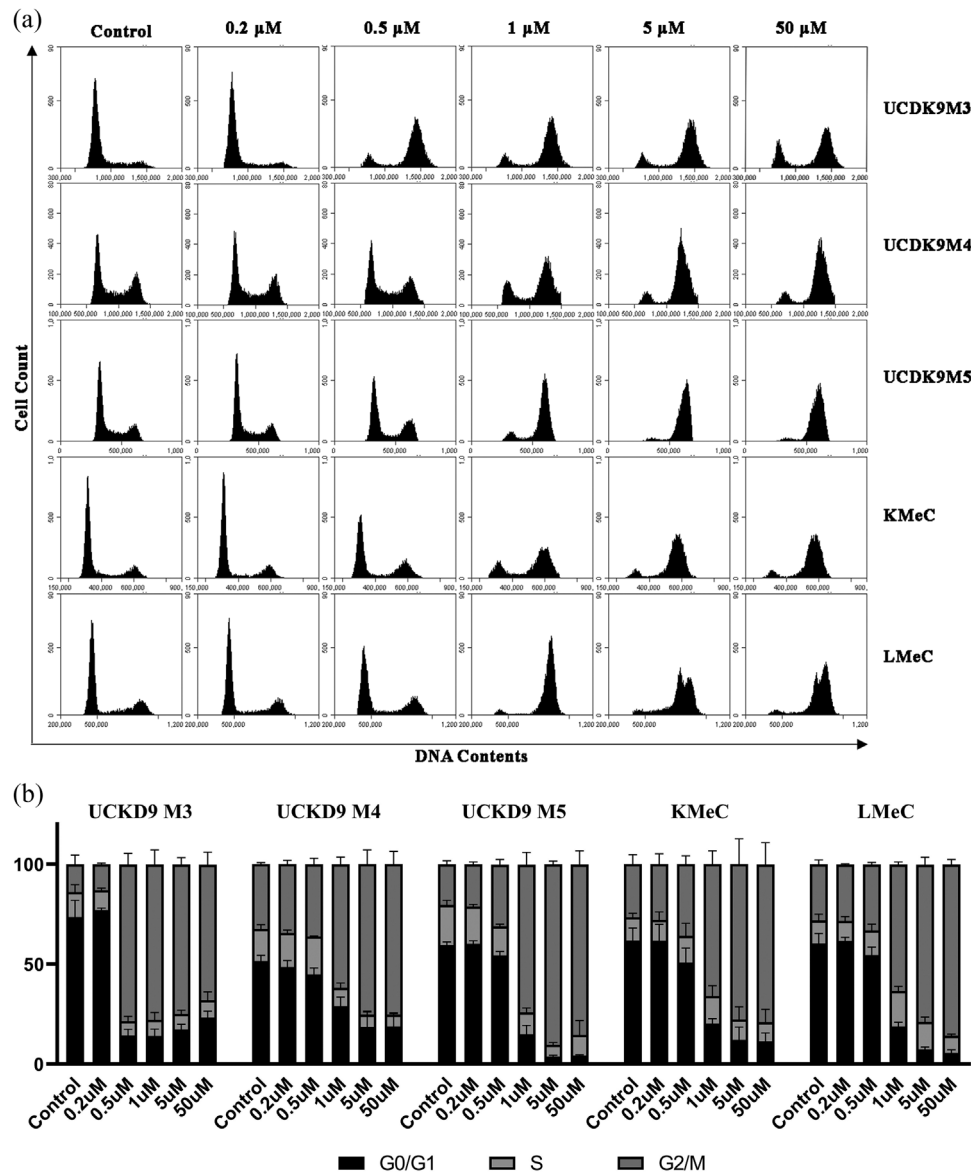


FIGURE 2 Cell cycle analysis with different FBZ concentrations and for different lengths of treatment. Cell count and DNA contents graphs show cell cycle shift (a). Stack-bar graph shows reduced G0/G1 phase and increased G2/M phase as treatment dose increases for the 24-h FBZ treatment (b). Extended gate of propidium iodide-height and propidium iodide-area shows cell cycle shift from G0/G1 to G2/M, split of cell population in G2/M and >4N population (c). Bar chart of cell cycle at different time periods at 0.5, 1 and 5 μM FBZ treatment (d). At 0.5 μM treatment, G2/M phase slightly increased at 8 h, but the cell cycle was restored after 8 h. Bar chart of sub-G1 and >4N fraction with various treatment concentrations (e). Bar chart of sub-G1 and >4N population (f); polyploid cells and sub-G1 cells are increased at 1 and 5 μM, but sub-G1 ratio of UCDK9M4 and UCDK9M5 cells at 1 μM is higher than at 5 μM (* $p < 0.05$, ** $p < 0.01$, Treatment vs. Control)

doses (UCDK9M4 at 0.5 μM, UCDK9M5 at 1 μM, KMeC at 1 μM and 5 μM and LMeC at 5 μM). The >4N population in the four cell lines showed a remarkable increase at 1 μM.

In the 48 h analysis with various time points, UCDK9M3, KMeC and LMeC exhibited an elevated sub-G1 ratio as the dose increased. UCDK9M4 and UCDK9M5 cells showed a lower sub-G1 population at 5 μM compared to the 1 μM treatment (Figure 2f, Table 4). Polyploid cells increased at 1 and 5 μM treatment, except for UCDK9M3 cells.

Analysis with flow cytometry confirmed that UCDK9M3 cells began to undergo apoptosis at lower FBZ concentrations and did not engage

in mitotic slippage. The other cell lines entered mitotic slippage at 1 μM treatment, but the tendency varied depending on the cell line.

3.4 | Apoptotic effect of FBZ

Since the cell cycle analysis showed that exposure to FBZ resulted in an increased sub-G1 population in canine melanoma cells, western blot was used to identify further evidence of apoptosis and to analyse the cell cycle. All of the 24-h treatment concentrations induced increased

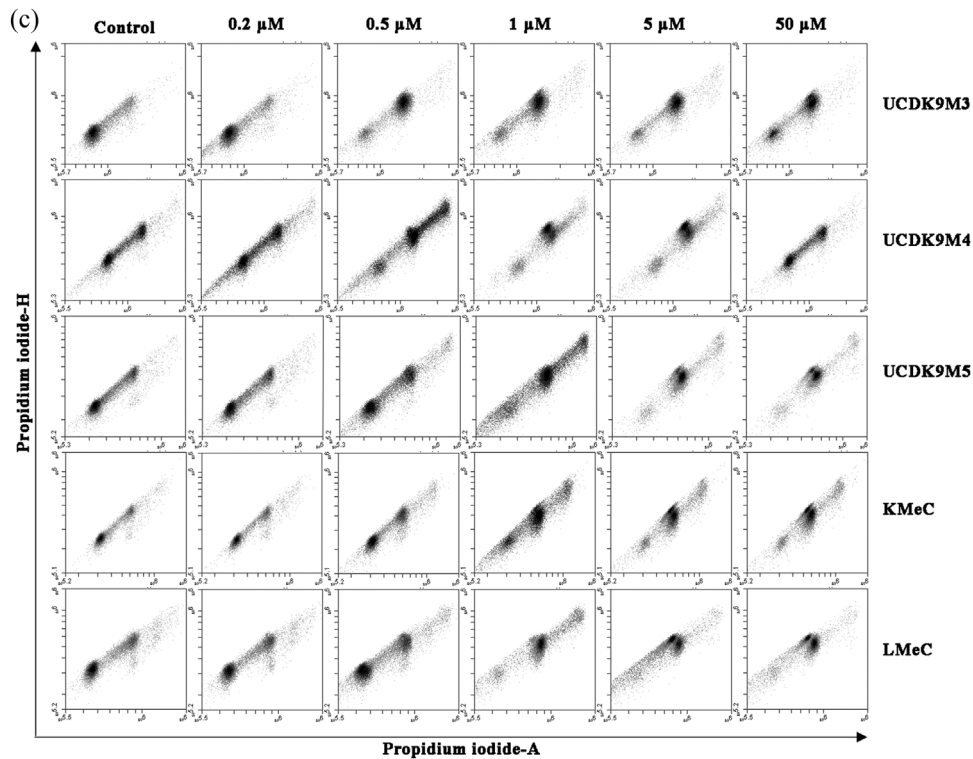


FIGURE 2 Continued

cleaved PARP levels compared to the control (Figure 3a). Over the time course of treatment for 48 h, all of the cell lines also exhibited increasing levels of cleaved PARP signal as time progressed.

Excluding UCDK9M3, the intensity of cyclinB1 was sustained over 8–32 h at a dose of 0.5 μ M FBZ, but cyclinB1 intensity at 1 and 5 μ M of FBZ increased early and exhibited a narrow time period (Figure 3b). The cyclinB1 signal in UCDK9M3 cells was much weaker than in the other cell lines and did not differ between treatment concentrations. This indicates that FBZ disrupts the cell cycle in melanoma cells by altering cyclinB1 levels and activity. In addition, since the UCDK9M3 cell line had reduced cyclinB1 levels compared to the other cell lines, this may explain why these cells did not undergo mitotic slippage.

3.5 | Anti-tubulin effect and mitotic slippage

Immunofluorescence microscopy for α -tubulin and DAPI counter staining showed anti-tubulin effects and dramatic morphologic changes in the microtubule cytoskeleton (Figure 4). All cell lines treated with FBZ underwent changes in cell shape from an angular morphology with a normal filamentous structure to rounded cytoplasmic margins with clumped tubulin. UCDK9M3 cells displayed shrunk cytoplasmic margins at doses higher than 0.5 μ M, but their nuclear shape and number did not change (Figure 4b–d). The other four cell lines showed multinucleation at doses of 0.5 and 1 μ M FBZ (Figure 4f, g, j, k, n, o, r and s). UCDK9M4 and UCDK9M5 cells showed macronucleation at

5 μ M FBZ treatment (Figure 4h and l), while KMeC and LMeC had markedly increased numbers of nuclei (Figure 4p and t).

4 | DISCUSSION

Currently, many attempts are being made to repurpose pre-existing drugs for anti-cancer effects. As part of that effort beta-tubulin inhibitors, including FBZ, have been recognised as potential chemotherapeutic agents, and studies have demonstrated that FBZ has anti-tubulin and cytotoxic effects (Doudican et al., 2008; Gao et al., 2008; Lai et al., 2017; Schmit, 2013). One such study discovered that FBZ could modulate multiple cellular pathways in human non-small cell lung carcinoma (A549 cells), including mitochondrial translocation of p53 and inhibition of glucose uptake. Mouse experiments in the same study showed growth inhibition of cancer cells with oral intake of the drug (Dogra et al., 2018). In veterinary medicine, FBZ has also been demonstrated to have an anti-tubulin effect on canine tumour cells (glioma and osteosarcoma), but few studies have examined the specific mechanism of this anti-cancer effect (Lai et al., 2017; Schmit, 2013). Thus, we conducted this study to uncover mechanisms of this anti-cancer effect and to understand the influence of FBZ on canine oral melanoma cells.

The cell viability, cell cycle arrest, apoptotic progression and morphology of five different canine malignant oral melanoma cells were assessed to evaluate the anti-cancer effects of FBZ at different treatment concentrations or for different treatment durations. Regarding

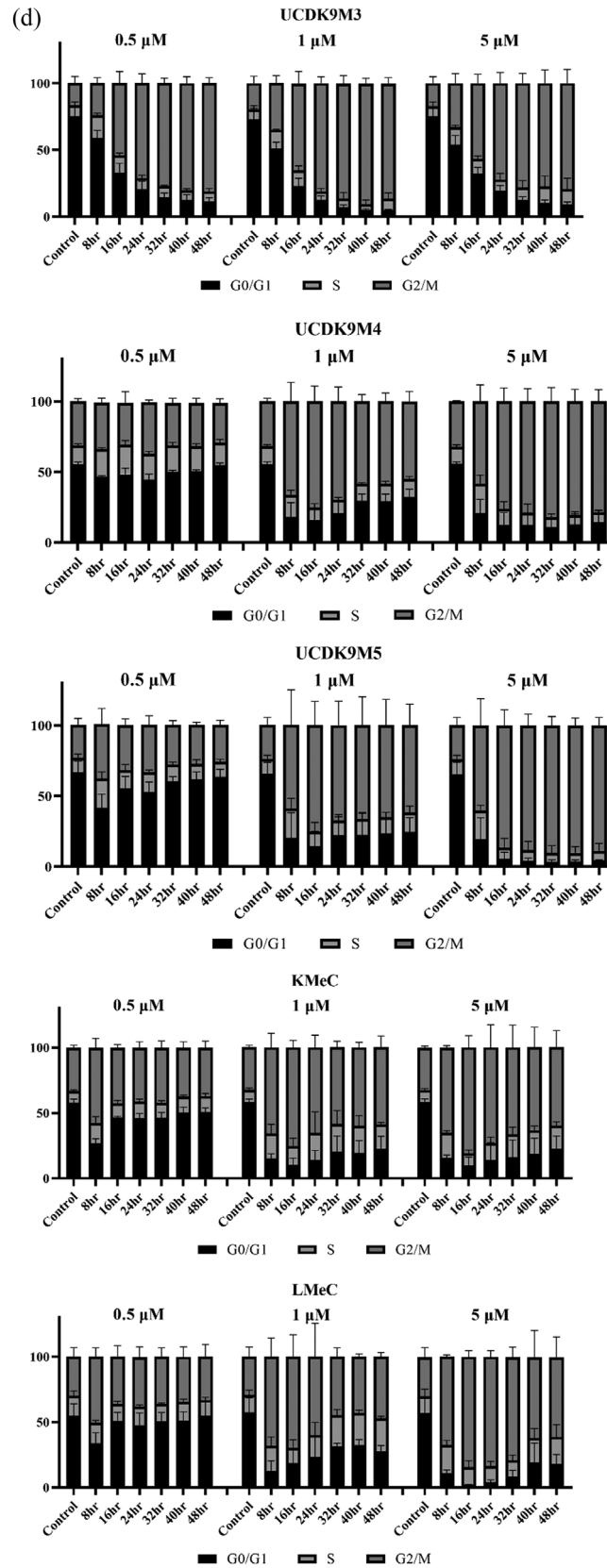


FIGURE 2 Continued

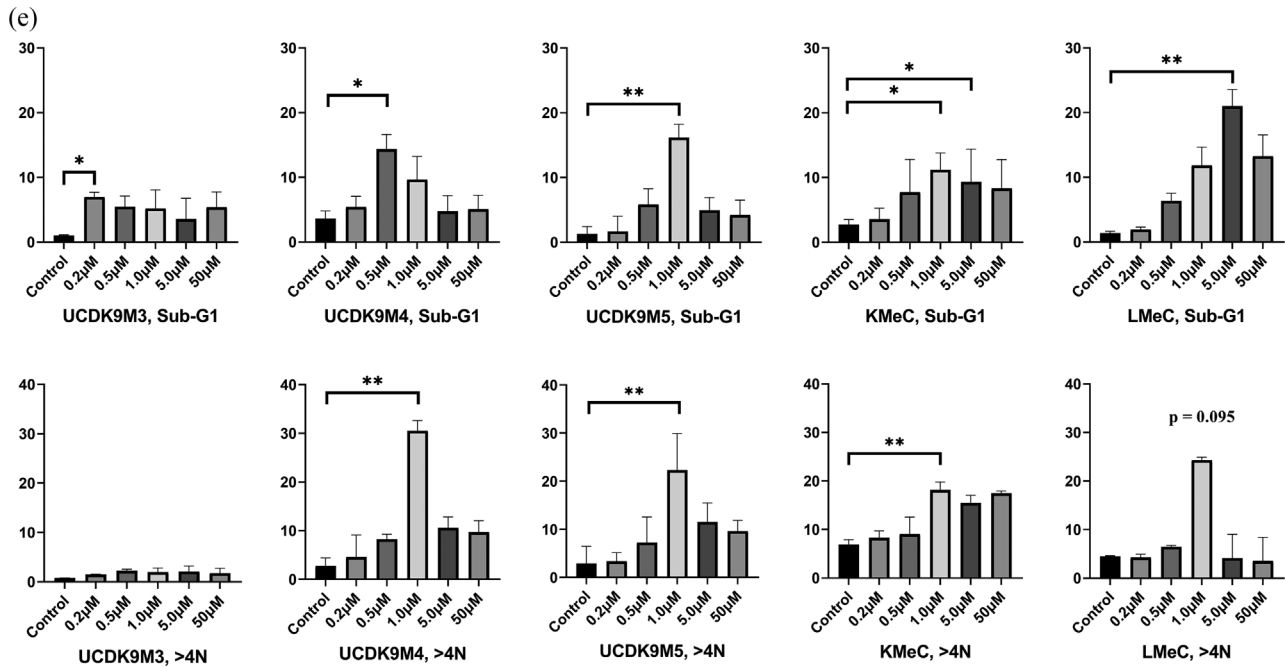


FIGURE 2 Continued

the sensitivity of canine melanoma to FBZ in this study, we found that the IC_{50} values ranged from 0.47 to 4.10 μM , which overlapped with the results of oral administration (C_{max} : 2.14 μM with 20 mg/kg for 5 consecutive days, and 1.57 μM with 20 mg/kg once) (McKellar et al., 1990; McKellar et al., 1993). It is notable that the concentrations of FBZ used in this study are achievable by oral administration in dogs.

This study showed FBZ induced G2/M arrest and increased tetraploid cells, along with evidence of apoptosis. When cancer cells are treated with MTAs, they can enter three possible conditions: (i) mitotic cell death, (ii) multi-nucleated tetraploid cells and post-slippage death or (iii) senescence escape (Cheng & Crasta, 2017). In addition, the term mitotic catastrophe is also used to describe more complicated cell fates. Although mitotic catastrophe is not fully understood, it is defined as cell death resulting from aberrant mitosis and may represent an oncosuppressive mechanism that is distinctive from apoptosis, necrosis or senescence (Portugal et al., 2009; Vitale et al., 2011). Based on our results, FBZ induced some cells to enter an apoptotic pathway, while other cells escaped senescence and became >4N cells. These results suggest that the cells underwent mitotic slippage and post-slippage cell death, indicative of mitotic catastrophe.

Interestingly, although the five melanoma cell lines were arrested in the G2/M phase, they exhibited distinct morphological changes at different treatment concentrations. UCDK9M3 cells showed G2/M arrest at 0.5 μM treatment, but it did not have mitotic slippage. The other four cell lines showed mitotic slippage and multinucleation at 1 μM . KMeC and LMeC showed multinucleation at 5 μM , but UCDK9M4 and UCDK9M5 showed macronucleation at the same concentration. During mitotic slippage, nuclear envelopes are randomly formed around groups of chromosomes, followed by chromosome decondensation, and the formation of multi-nucleated cells

(Blagosklonny, 2007). Chromosomes are segregated by mitotic spindles and there are many of possible pathways for cells to become multi-nucleated or macronucleated (Vitale et al., 2011). Based on the effects of MTAs, mitotic spindle disruption generates tetraploid cells, and tetraploid cells with multipolar spindles can progress to multi-nuclear or octoploid states, which are described as macronucleated (Vitale et al., 2011). Therefore, it can be speculated that some concentrations of FBZ treatment, such as 5 μM in UCDK9M4 and UCDK9M5 cells, may alter the effect of FBZ on mitotic spindle dynamics, leading to macronucleation.

From the western blot analysis of cleaved PARP, FBZ treatment resulted in apoptosis, along with an increased sub-G1 population in a time-dependent manner. However, UCDK9M4 and UCDK9M5 cells, which showed macronucleation, exhibited reduced numbers of sub-G1 cells at 5 μM compared to 1 μM , but KMeC and LMeC did not exhibit a decreased number of sub-G1 cells at 5 μM . This result indicates that macronucleation may be correlated with a decreased sub-G1 population and different FBZ concentrations can result in different consequences. However, the precise molecular mechanism driving mitotic catastrophe and the distinct cellular consequences for multinucleation and micronucleation are unclear.

From cell culture studies, the main target of MTAs is rapidly dividing cells (Jordan & Kamath, 2007). During mitosis, especially in the progression from pro-metaphase to anaphase, spindle assembly checkpoint (SAC) plays an important role. Prolonged SAC activation causes mitotic arrest and often, but not in all cases, mitotic catastrophe (Vitale et al., 2011). One study analysed the correlation between SAC incompleteness and aneuploidy in canine melanoma cells treated with nocodazole, an MTA, and found that a defect in a SAC component is correlated with aneuploidy in canine melanoma cells

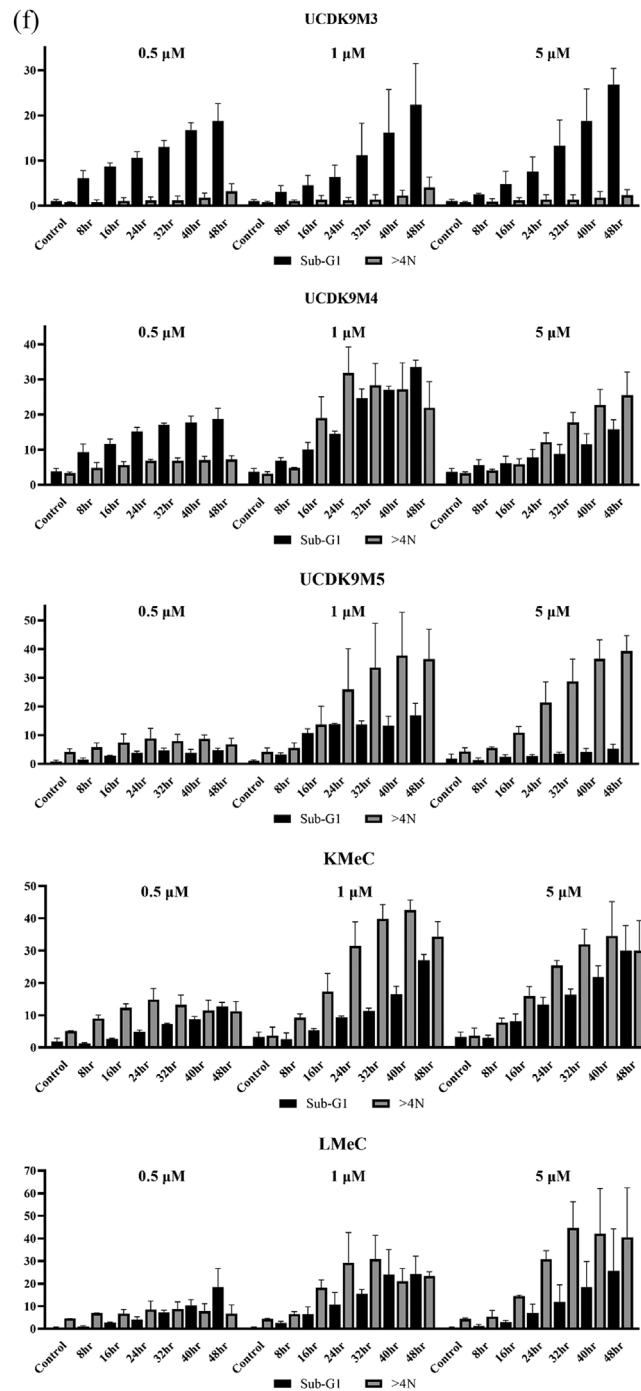


FIGURE 2 Continued

(Endo et al., 2020). In addition to SAC, many of other cellular proteins, including anaphase-promoting complex (APC) and cyclin B1/Cdk1 complex, were shown to have an important role during mitosis and mitotic slippage (Cheng & Crasta, 2017). Cells in G2 phase require cyclin B1/Cdk1 complex activation to enter mitosis, and cyclin B1 must be degraded by APC for mitotic exit (DiPaola, 2002; Lara-Gonzalez et al., 2012; Rieder & Maiato, 2004). Under normal circumstances, SAC inhibits improper chromosome separation and mitotic exit by inhibiting APC. MTAs, however, disturb microtubule dynamics by sustaining

SAC, which down regulates APC. This leads to a lack of degradation of cyclin B1, preventing cancer cells from exiting mitosis. On the other hand, when SAC is not sufficiently sustained, APC can function normally, which promotes the slow degradation of cyclin B1 and mitotic slippage. In our western blot analysis at various time points of treatment, with the exception of UCCK9M3, the intensity of cyclin B1 at 1 or 5 μM was increased early and at higher levels than at 0.5 μM , but this increase was transient. Since FBZ treatment at 1 or 5 μM did not produce a prolonged cyclin B1 increase, the four melanoma cell

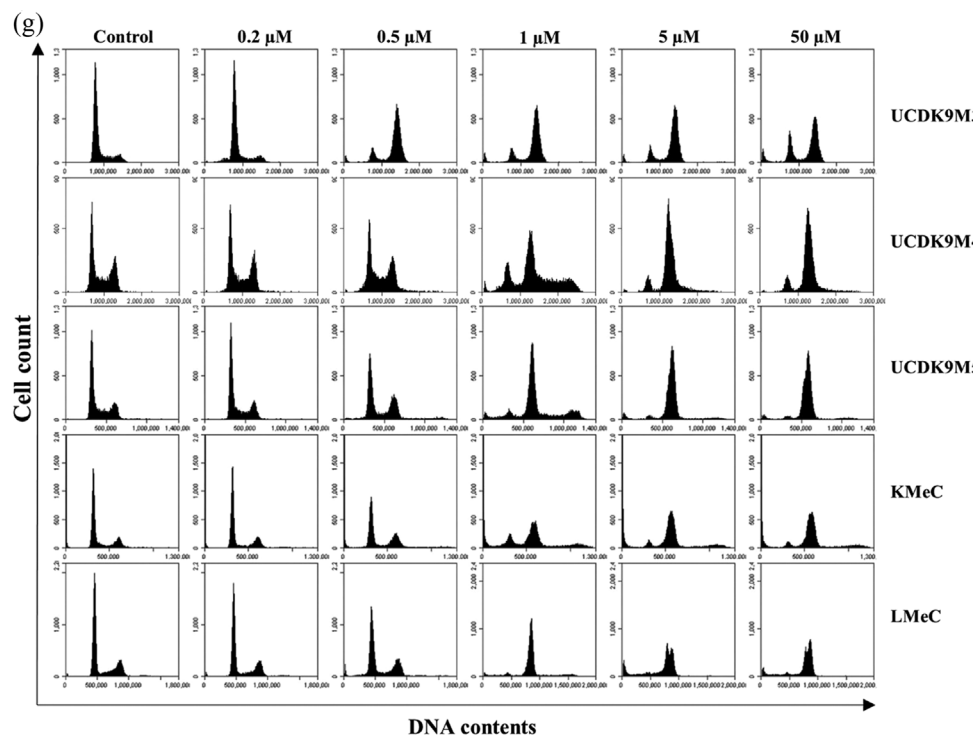


FIGURE 2 Continued

TABLE 1 FBZ treatment for 24 h

		Control	0.2 μ M	0.5 μ M	1 μ M	5 μ M	50 μ M
UCDK9M3	G0/G1	73.64 \pm 8.29	77.11 \pm 1.02	14.27 \pm 3.20	14.07 \pm 3.47	17.36 \pm 2.57	23.35 \pm 3.16
	S	12.43 \pm 3.68	9.90 \pm 1.07	7.24 \pm 2.45	8.02 \pm 3.81	7.64 \pm 1.98	8.64 \pm 4.11
	G2/M	13.90 \pm 4.63	12.91 \pm 0.61	78.28 \pm 5.66	77.73 \pm 7.30	74.83 \pm 3.41	67.77 \pm 6.23
UCDK9M4	G0/G1	51.53 \pm 2.85	48.60 \pm 3.33	44.90 \pm 3.19	28.97 \pm 4.66	18.60 \pm 7.41	18.82 \pm 6.44
	S	16.09 \pm 2.17	17.00 \pm 1.47	19.00 \pm 0.21	9.23 \pm 2.42	6.13 \pm 1.72	5.92 \pm 0.92
	G2/M	32.37 \pm 0.84	34.41 \pm 1.95	36.05 \pm 3.02	61.77 \pm 3.58	75.29 \pm 7.10	75.25 \pm 6.42
UCDK9M5	G0/G1	59.53 \pm 1.63	60.17 \pm 1.55	54.40 \pm 1.91	14.95 \pm 4.39	3.74 \pm 0.63	4.36 \pm 0.35
	S	20.12 \pm 2.35	18.65 \pm 1.13	14.51 \pm 1.11	10.89 \pm 2.27	5.84 \pm 1.24	10.18 \pm 7.29
	G2/M	20.29 \pm 1.83	21.14 \pm 1.21	30.86 \pm 2.64	73.85 \pm 6.28	90.36 \pm 1.65	85.30 \pm 6.90
KMeC	G0/G1	61.87 \pm 6.26	61.70 \pm 8.27	50.74 \pm 7.37	20.26 \pm 2.40	12.09 \pm 6.49	11.30 \pm 4.30
	S	11.61 \pm 1.92	10.44 \pm 3.99	13.39 \pm 6.31	13.84 \pm 5.21	10.25 \pm 6.34	9.68 \pm 6.37
	G2/M	26.50 \pm 4.78	27.88 \pm 5.24	35.86 \pm 4.20	65.89 \pm 6.72	77.69 \pm 12.76	78.86 \pm 10.94
LMeC	G0/G1	60.30 \pm 5.14	61.62 \pm 1.86	54.55 \pm 4.04	18.89 \pm 2.12	7.38 \pm 1.25	5.50 \pm 1.63
	S	11.57 \pm 3.17	10.11 \pm 2.04	12.38 \pm 3.10	17.62 \pm 2.34	13.70 \pm 2.39	8.65 \pm 0.79
	G2/M	28.08 \pm 2.23	28.09 \pm 0.46	32.88 \pm 1.12	63.35 \pm 1.33	78.61 \pm 3.81	85.67 \pm 2.51

Note: The table shows the percentage of G0/G1, S and G2/M phase cells in five melanoma cell lines. Data are presented as mean \pm standard deviation. FBZ, fenbendazole.

lines may have been unable to regulate spindle assembly disruptions. This suppressed function may explain why some of the cells arrested in G2/M phase, while others progressed into mitotic slippage with disturbed mitotic dynamics. Moreover, UCDK9M3 did not exhibit changes in cyclin B1 concentration between treatment concentrations, which may be related to the lack of mitotic slippage in these cells.

In addition to the effect of MTAs on mitosis, some research suggests mitosis-independent toxicity as well. A study of human breast carcinoma cells showed that treatment with anti-tubulin agents (nocodazole, vincristine and taxol) induced an apoptotic effect not only in polyploid cells, but also mononuclear cells that do not enter mitosis (Kisurina-Evgen'eva et al., 2006). The microtubule cytoskeleton plays

TABLE 2 FBZ treatment and analysis at different time points

			Control	8 h	16 h	24 h	32 h	40 h	48 h
UCDK9 M3	0.5 μ M	G0/G1	75.43 \pm 6.90	59.16 \pm 5.46	32.92 \pm 7.10	20.69 \pm 5.94	14.52 \pm 3.29	12.75 \pm 3.79	11.45 \pm 2.85
		S	8.09 \pm 2.49	16.85 \pm 1.69	13.19 \pm 1.64	8.19 \pm 2.21	8.58 \pm 0.48	7.04 \pm 1.20	7.55 \pm 2.22
		G2/M	16.58 \pm 4.97	24.20 \pm 3.85	54.04 \pm 8.52	71.23 \pm 6.90	77.01 \pm 3.74	80.25 \pm 4.96	81.12 \pm 3.99
	1 μ M	G0/G1	73.09 \pm 8.14	50.98 \pm 4.87	23.21 \pm 5.58	12.64 \pm 3.06	7.26 \pm 1.57	5.07 \pm 1.00	4.98 \pm 0.36
		S	7.22 \pm 2.93	14.09 \pm 0.50	11.56 \pm 3.34	6.36 \pm 2.18	6.45 \pm 4.39	4.51 \pm 3.04	8.61 \pm 4.29
		G2/M	19.74 \pm 5.24	35.09 \pm 5.47	65.06 \pm 9.02	80.96 \pm 4.89	86.16 \pm 5.73	90.20 \pm 3.92	86.19 \pm 4.39
	5 μ M	G0/G1	75.32 \pm 7.20	54.07 \pm 6.91	32.33 \pm 4.73	19.61 \pm 3.75	12.67 \pm 2.21	10.27 \pm 2.36	9.28 \pm 1.79
		S	7.45 \pm 3.11	12.97 \pm 1.49	11.07 \pm 2.10	8.25 \pm 4.54	9.14 \pm 5.26	12.51 \pm 7.93	11.32 \pm 8.28
		G2/M	17.2 \pm 5.01	32.96 \pm 7.10	56.59 \pm 6.75	72.16 \pm 8.02	78.14 \pm 7.36	77.19 \pm 9.94	79.4 \pm 10.32
UCDK9 M4	0.5 μ M	G0/G1	55.61 \pm 1.51	46.76 \pm 0.64	48.24 \pm 4.47	44.68 \pm 3.82	50.11 \pm 1.17	50.62 \pm 0.98	54.73 \pm 1.72
		S	13.13 \pm 1.18	19.32 \pm 1.11	21.04 \pm 3.04	18.39 \pm 1.65	18.66 \pm 2.26	17.58 \pm 1.91	16.07 \pm 2.32
		G2/M	31.39 \pm 1.90	32.99 \pm 3.22	29.64 \pm 7.98	36.43 \pm 1.48	30.02 \pm 3.38	30.54 \pm 3.46	28.04 \pm 3.09
	1 μ M	G0/G1	55.3 \pm 1.90	18.18 \pm 10.12	16.05 \pm 8.47	21.04 \pm 8.76	29.68 \pm 4.76	29.24 \pm 5.07	32.39 \pm 5.44
		S	13.04 \pm 1.10	15.52 \pm 3.42	8.75 \pm 2.90	9.23 \pm 1.73	11.91 \pm 0.80	12.42 \pm 1.81	12.56 \pm 1.91
		G2/M	31.77 \pm 2.11	66.44 \pm 13.38	75.31 \pm 10.83	69.85 \pm 10.08	58.55 \pm 4.73	58.40 \pm 5.89	55.09 \pm 7.01
	5 μ M	G0/G1	55.80 \pm 1.23	20.99 \pm 9.61	12.64 \pm 8.52	12.56 \pm 8.40	11.01 \pm 9.29	12.82 \pm 7.33	14.32 \pm 8.25
		S	11.92 \pm 1.56	20.77 \pm 6.07	11.09 \pm 5.22	8.58 \pm 6.26	6.96 \pm 2.25	6.46 \pm 2.52	7.16 \pm 1.42
		G2/M	32.39 \pm 0.48	58.45 \pm 11.57	76.44 \pm 9.31	78.97 \pm 8.89	82.15 \pm 9.64	80.86 \pm 8.49	78.64 \pm 8.26
UCDK9 M5	0.5 μ M	G0/G1	66.87 \pm 7.67	41.61 \pm 9.77	55.41 \pm 8.49	52.87 \pm 7.1	60.53 \pm 3.26	61.93 \pm 5.12	63.72 \pm 5.21
		S	10.26 \pm 2.63	20.80 \pm 4.70	12.75 \pm 4.10	14.17 \pm 1.40	11.75 \pm 1.85	10.68 \pm 3.16	10.61 \pm 1.70
		G2/M	23.15 \pm 4.70	38.38 \pm 11.35	32.1 \pm 4.44	33.55 \pm 6.19	28.14 \pm 3.02	27.72 \pm 1.82	26.12 \pm 3.17
	1 μ M	G0/G1	65.75 \pm 8.03	20.58 \pm 17.63	14.73 \pm 10.27	22.39 \pm 12.87	22.70 \pm 15.86	23.73 \pm 14.87	24.70 \pm 10.04
		S	10.53 \pm 2.60	20.79 \pm 6.97	10.09 \pm 6.50	10.35 \pm 4.19	10.89 \pm 4.15	11.30 \pm 3.39	13.73 \pm 4.44
		G2/M	24.05 \pm 5.36	59.00 \pm 24.84	75.36 \pm 16.9	67.41 \pm 17.04	66.58 \pm 20.13	65.17 \pm 18.33	61.82 \pm 14.71
	5 μ M	G0/G1	65.51 \pm 8.41	19.40 \pm 15.25	5.72 \pm 4.60	3.98 \pm 2.11	3.49 \pm 1.36	3.90 \pm 0.87	4.48 \pm 0.26
		S	10.51 \pm 2.76	20.24 \pm 3.75	7.82 \pm 6.51	8.01 \pm 6.01	6.36 \pm 5.07	5.86 \pm 4.46	6.56 \pm 5.47
		G2/M	24.2 \pm 5.48	60.35 \pm 18.89	86.43 \pm 11.08	87.99 \pm 8.04	90.14 \pm 6.38	90.26 \pm 5.30	88.95 \pm 5.72
KMeC	0.5 μ M	G0/G1	58.06 \pm 2.59	26.91 \pm 3.38	46.88 \pm 0.57	45.98 \pm 3.62	46.36 \pm 4.10	50.34 \pm 4.18	50.78 \pm 3.05
		S	8.79 \pm 0.76	15.45 \pm 4.87	10.54 \pm 2.14	12.72 \pm 1.91	11.38 \pm 1.62	12.08 \pm 1.26	12.04 \pm 2.03
		G2/M	33.15 \pm 1.84	57.40 \pm 7.25	42.59 \pm 2.31	41.31 \pm 4.55	42.28 \pm 5.01	37.59 \pm 4.55	37.19 \pm 4.88
	1 μ M	G0/G1	58.22 \pm 2.43	14.99 \pm 3.90	10.41 \pm 5.03	14.38 \pm 6.90	20.7 \pm 11.70	19.41 \pm 9.50	22.95 \pm 9.40
		S	9.44 \pm 1.45	19.45 \pm 6.90	14.15 \pm 6.16	20.49 \pm 16.02	20.88 \pm 10.28	20.72 \pm 7.77	18.27 \pm 1.63
		G2/M	32.54 \pm 1.61	65.70 \pm 10.92	75.51 \pm 5.56	65.26 \pm 9.35	58.6 \pm 4.52	60.02 \pm 3.94	58.99 \pm 8.67
	5 μ M	G0/G1	58.27 \pm 2.39	15.84 \pm 2.07	9.90 \pm 6.42	14.38 \pm 12.98	16.46 \pm 13.01	18.83 \pm 11.95	22.64 \pm 9.81
		S	9.24 \pm 1.15	19.10 \pm 1.55	9.29 \pm 2.41	12.63 \pm 4.42	17.24 \pm 5.60	17.91 \pm 3.36	17.69 \pm 3.03
		G2/M	32.43 \pm 1.19	65.04 \pm 1.60	80.93 \pm 8.93	73.12 \pm 17.22	66.45 \pm 17.08	63.46 \pm 15.33	59.86 \pm 12.77
LMeC	0.5 μ M	G0/G1	54.75 \pm 9.27	33.86 \pm 8.17	50.93 \pm 6.62	47.68 \pm 9.29	50.65 \pm 6.74	51.23 \pm 6.75	54.86 \pm 10.91
		S	15.34 \pm 3.67	15.78 \pm 1.75	12.91 \pm 2.19	14.28 \pm 1.30	13.23 \pm 0.83	14.42 \pm 2.03	12.10 \pm 1.99
		G2/M	30.04 \pm 6.76	50.57 \pm 6.60	36.25 \pm 8.30	37.85 \pm 7.82	36.14 \pm 6.79	34.20 \pm 7.81	33.15 \pm 9.29
	1 μ M	G0/G1	57.34 \pm 11.38	13.01 \pm 7.39	18.59 \pm 10.72	23.53 \pm 15.92	31.44 \pm 2.45	32.40 \pm 4.30	27.63 \pm 4.44
		S	13.34 \pm 3.89	18.86 \pm 6.85	11.86 \pm 6.02	16.61 \pm 9.72	23.82 \pm 4.39	24.64 \pm 2.14	25.36 \pm 1.42
		G2/M	29.33 \pm 7.50	68.11 \pm 14.24	69.57 \pm 16.67	59.87 \pm 25.62	44.75 \pm 6.81	42.95 \pm 2.23	46.99 \pm 3.3
	5 μ M	G0/G1	57.05 \pm 10.96	10.98 \pm 2.55	2.22 \pm 0.17	4.13 \pm 1.71	8.73 \pm 4.52	19.39 \pm 14.71	18.33 \pm 6.91
		S	12.63 \pm 5.41	21.57 \pm 3.44	13.50 \pm 4.86	12.26 \pm 3.55	12.28 \pm 3.85	18.69 \pm 7.08	20.25 \pm 9.61
		G2/M	30.12 \pm 7.12	67.42 \pm 1.35	84.23 \pm 4.64	83.52 \pm 4.72	78.80 \pm 7.47	61.57 \pm 20.43	60.88 \pm 15.59

Note: The table shows the percentage of G0/G1, S and G2/M phase cells in five melanoma cell lines

TABLE 3 FBZ treatment for 24 h

		Control	0.2 μ M	0.5 μ M	1 μ M	5 μ M	50 μ M
UCDK9M3	sub-G1	0.87 \pm 0.37	6.50 \pm 1.52*	5.47 \pm 1.67	6.09 \pm 1.73	4.56 \pm 1.93	5.63 \pm 2.03
	>4N	0.76 \pm 0.03	1.27 \pm 0.43	2.14 \pm 0.46	2.23 \pm 0.50	2.33 \pm 0.77	2.02 \pm 0.62
UCDK9M4	sub-G1	3.95 \pm 0.76	5.75 \pm 1.20	13.64 \pm 3.41*	10.32 \pm 2.64	5.50 \pm 1.45	5.47 \pm 1.60
	>4N	3.32 \pm 0.94	5.82 \pm 2.90	7.91 \pm 1.60	26.63 \pm 5.24**	10.20 \pm 2.86	9.53 \pm 2.64
UCDK9M5	sub-G1	1.66 \pm 0.66	2.35 \pm 1.48	6.17 \pm 1.95	13.80 \pm 5.97**	5.54 \pm 1.18	4.71 \pm 1.61
	>4N	3.98 \pm 2.17	3.81 \pm 1.21	8.94 \pm 3.18	24.55 \pm 4.70**	11.82 \pm 3.53	9.37 \pm 2.67
KMeC	sub-G1	2.65 \pm 0.91	3.55 \pm 1.73	8.46 \pm 4.03	11.26 \pm 2.53*	10.84 \pm 3.09*	9.48 \pm 2.91
	>4N	6.62 \pm 1.43	7.74 \pm 2.30	9.90 \pm 2.35	18.42 \pm 1.25**	15.07 \pm 2.18	15.91 \pm 3.14
LMeC	sub-G1	1.13 \pm 0.67	1.78 \pm 0.63	6.57 \pm 0.90	12.15 \pm 2.38	20.74 \pm 2.98**	14.16 \pm 2.09*
	>4N	4.32 \pm 0.45	4.33 \pm 0.59	6.22 \pm 0.66	22.94 \pm 2.95	5.49 \pm 3.11	4.86 \pm 3.10

Note: Sub-G1 and >4N cells from cell cycle analysis data are presented as a percentage and mean \pm standard deviation. Kruskal–Wallis test was used to calculate the significance with Dunn's multiple comparison test (bold * p < 0.05, ** p < 0.01, Treatment vs. Control)

TABLE 4 FBZ treatment and Sub-G1 and >4N cell populations at different time points

			Control	8 h	16 h	24 h	32 h	40 h	48 h
UCDK9 M3	0.5 μ M	Sub-G1	1.11 \pm 0.29	6.14 \pm 1.68	8.68 \pm 0.81	10.59 \pm 1.39	12.99 \pm 1.46	16.82 \pm 1.53	18.76 \pm 3.85
		>4N	0.78 \pm 0.15	0.84 \pm 0.48	1.11 \pm 0.69	1.19 \pm 0.75	1.19 \pm 0.98	1.82 \pm 1.01	3.18 \pm 1.69
	1 μ M	Sub-G1	1.07 \pm 0.29	3.10 \pm 1.38	4.56 \pm 2.17	6.31 \pm 2.68	11.17 \pm 7.11	16.12 \pm 9.58	22.35 \pm 9.13
		>4N	0.81 \pm 0.21	1.04 \pm 0.27	1.35 \pm 0.90	1.19 \pm 0.63	1.42 \pm 1.04	2.25 \pm 1.18	4.01 \pm 2.36
	5 μ M	Sub-G1	1.09 \pm 0.32	2.48 \pm 0.28	4.79 \pm 2.83	7.52 \pm 3.32	13.34 \pm 5.66	18.79 \pm 7.06	26.78 \pm 3.63
		>4N	0.78 \pm 0.16	0.94 \pm 0.62	1.23 \pm 0.57	1.39 \pm 1.06	1.33 \pm 1.09	1.81 \pm 1.32	2.35 \pm 1.19
UCDK9 M4	0.5 μ M	Sub-G1	3.81 \pm 0.88	9.35 \pm 2.28	11.63 \pm 1.41	15.14 \pm 1.24	17.13 \pm 0.49	17.73 \pm 1.86	18.76 \pm 3.04
		>4N	3.32 \pm 0.35	4.84 \pm 1.53	5.64 \pm 1.01	6.90 \pm 0.37	6.89 \pm 0.80	7.10 \pm 1.03	7.21 \pm 1.14
	1 μ M	Sub-G1	3.78 \pm 0.91	6.86 \pm 0.91	10.11 \pm 2.00	14.54 \pm 0.75	24.69 \pm 2.60	27.12 \pm 0.99	33.51 \pm 1.99
		>4N	3.20 \pm 0.57	4.77 \pm 0.25	19.00 \pm 6.06	31.87 \pm 7.38	28.37 \pm 6.18	27.21 \pm 7.58	21.94 \pm 7.42
	5 μ M	Sub-G1	3.70 \pm 0.98	5.60 \pm 1.62	6.16 \pm 2.01	7.73 \pm 2.33	8.82 \pm 2.71	11.54 \pm 3.05	15.83 \pm 2.71
		>4N	3.28 \pm 0.44	4.04 \pm 0.45	5.87 \pm 1.57	12.12 \pm 2.70	17.81 \pm 2.80	22.69 \pm 4.49	25.46 \pm 6.64
UCDK9 M5	0.5 μ M	Sub-G1	0.90 \pm 0.40	1.57 \pm 0.53	2.83 \pm 0.16	3.89 \pm 0.57	4.76 \pm 0.77	3.91 \pm 1.18	4.79 \pm 0.70
		>4N	4.14 \pm 1.18	5.86 \pm 1.51	7.48 \pm 2.97	8.91 \pm 3.46	7.95 \pm 2.37	8.63 \pm 1.47	6.87 \pm 2.12
	1 μ M	Sub-G1	1.12 \pm 0.27	3.28 \pm 0.57	10.68 \pm 1.54	13.81 \pm 0.34	13.67 \pm 1.31	13.33 \pm 3.27	16.92 \pm 4.21
		>4N	4.22 \pm 1.35	5.66 \pm 1.65	13.69 \pm 6.39	25.94 \pm 14.13	33.55 \pm 15.44	37.74 \pm 15.08	36.52 \pm 10.39
	5 μ M	Sub-G1	1.85 \pm 1.61	1.34 \pm 0.77	2.46 \pm 0.82	2.79 \pm 0.55	3.56 \pm 0.53	4.19 \pm 1.18	5.27 \pm 1.53
		>4N	4.31 \pm 1.29	5.67 \pm 0.28	10.88 \pm 2.18	21.32 \pm 7.26	28.71 \pm 7.79	36.55 \pm 6.63	39.25 \pm 5.46
KMeC	0.5 μ M	Sub-G1	1.85 \pm 1.05	1.24 \pm 0.25	2.69 \pm 0.22	4.88 \pm 0.58	7.26 \pm 0.26	8.66 \pm 0.93	12.71 \pm 1.27
		>4N	5.10 \pm 0.13	9.02 \pm 1.04	12.32 \pm 1.24	14.85 \pm 3.48	13.23 \pm 3.02	11.47 \pm 3.16	11.23 \pm 3.06
	1 μ M	Sub-G1	3.25 \pm 1.55	2.61 \pm 1.91	5.35 \pm 0.55	9.37 \pm 0.37	11.32 \pm 0.87	16.48 \pm 2.51	27.03 \pm 1.82
		>4N	3.73 \pm 2.57	9.27 \pm 1.12	17.31 \pm 5.66	31.47 \pm 7.45	39.82 \pm 4.40	42.56 \pm 3.07	34.37 \pm 4.61
	5 μ M	Sub-G1	3.25 \pm 1.55	2.93 \pm 0.94	8.20 \pm 2.18	13.24 \pm 2.3	16.34 \pm 1.81	21.83 \pm 3.53	29.94 \pm 7.85
		>4N	3.59 \pm 2.45	7.73 \pm 1.39	15.88 \pm 3.02	25.42 \pm 1.56	31.92 \pm 4.71	34.60 \pm 10.59	29.94 \pm 9.35
LMeC	0.5 μ M	Sub-G1	0.54 \pm 0.30	0.98 \pm 0.37	2.82 \pm 0.22	4.25 \pm 1.10	7.20 \pm 0.99	10.38 \pm 2.59	18.42 \pm 8.31
		>4N	4.52 \pm 0.07	6.91 \pm 0.14	6.74 \pm 1.87	8.51 \pm 3.77	8.78 \pm 3.18	7.81 \pm 3.29	6.80 \pm 3.79
	1 μ M	Sub-G1	0.57 \pm 0.27	2.62 \pm 0.67	6.57 \pm 3.12	10.71 \pm 5.35	15.44 \pm 1.98	23.91 \pm 11.23	24.29 \pm 7.80
		>4N	4.37 \pm 0.31	6.50 \pm 1.09	18.20 \pm 3.47	29.27 \pm 13.42	30.87 \pm 10.46	21.15 \pm 5.61	23.3 \pm 1.94
	5 μ M	Sub-G1	0.53 \pm 0.31	1.33 \pm 0.54	2.87 \pm 0.86	6.85 \pm 4.10	11.80 \pm 7.68	18.39 \pm 11.44	25.66 \pm 18.63
		>4N	4.36 \pm 0.39	5.41 \pm 2.72	14.48 \pm 0.49	30.73 \pm 3.90	44.61 \pm 11.68	42.10 \pm 20.08	40.53 \pm 21.94

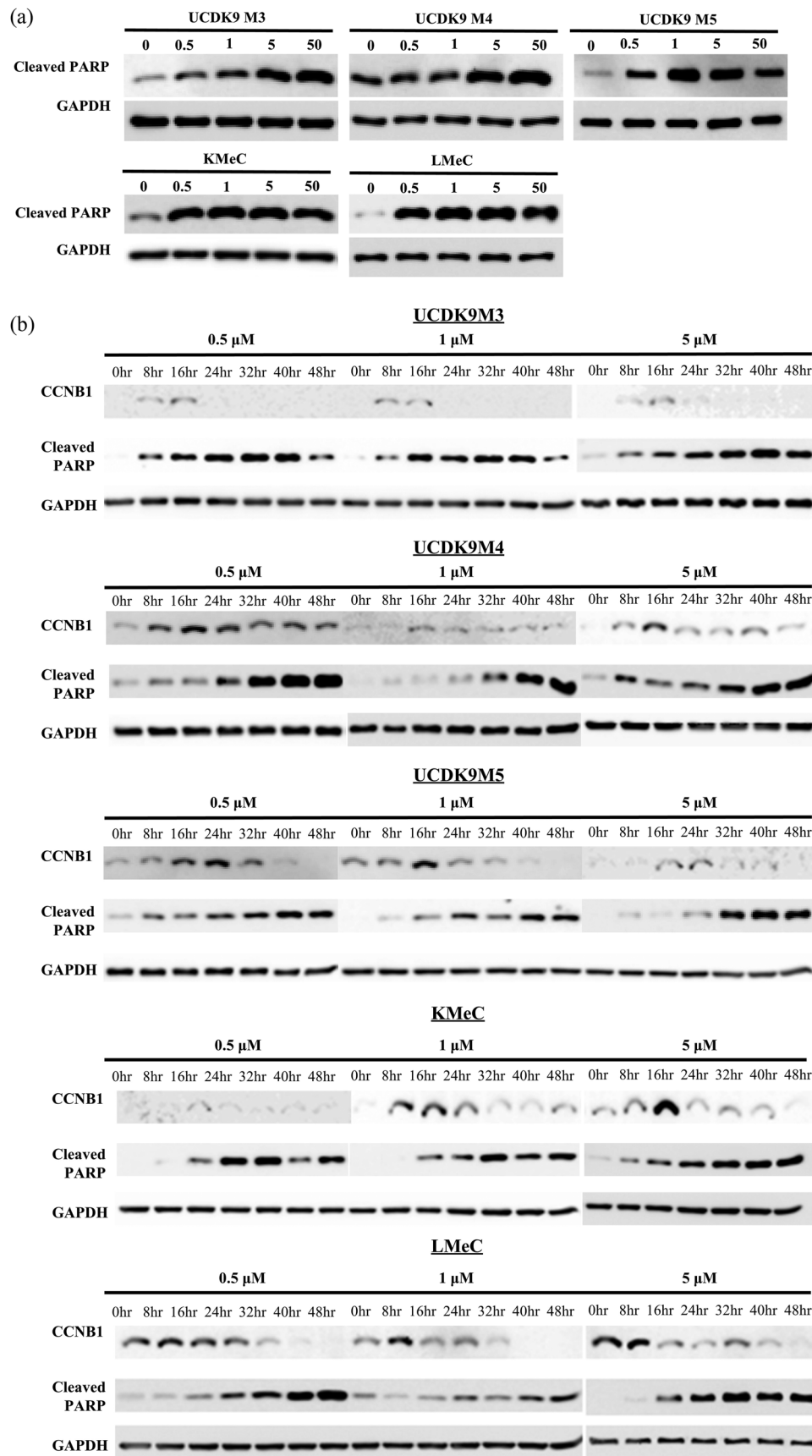


FIGURE 3 Western blot analysis of cleaved PARP. (a) Cleaved PARP at different concentrations for 24-h treatment. (b) Cleaved PARP and cyclinB1 over time

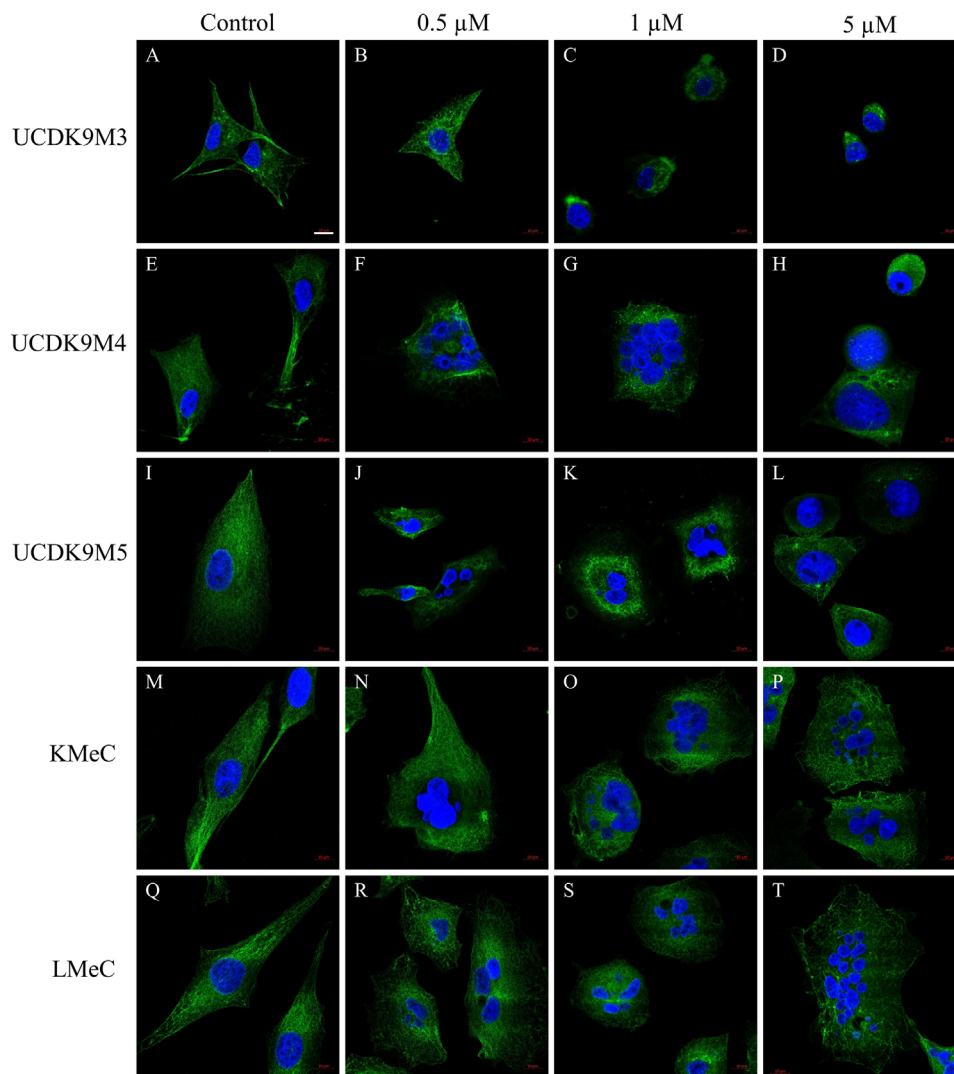


FIGURE 4 Immunofluorescence to examine cell morphology and mitotic slippage. Melanoma cells with no treatment show normal tubulin structure and cell shape; UCDK9M3 (a) UCDK9M4 (e), UCDK9M5 (i), KMeC (m) and LMeC (q). Treated UCDK9M3 cells show clumped tubulin structures at 0.5 μM (b) and reduced and rounded cytoplasmic morphology with normal nuclei at 1 μM (c) and 5 μM (d). UCDK9M4 cells shows similar clumping of tubulin and multinucleation at 0.5 μM (f) and at 1 μM (g), while UCDK9M4 cells exposed to 5 μM FBZ exhibit macronucleation. UCDK9M5 cells show the same pattern as UCDK9M4; clumping of tubulin and multinucleation at 0.5 μM (j) and 1 μM (k), macronucleation at 5 μM (l). KMeC and LMeC showed similar patterns, while higher concentrations intensified multinucleation (n) to (p) and (r) to (t). Mouse monoclonal alpha-tubulin primary antibody and FITC secondary antibody, DAPI counter stain. Bar = 10 μM

an important role in intracellular trafficking of oncoproteins, especially in cancer cells, and alterations in cell signalling and trafficking can induce apoptosis (Komlodi-Pasztor et al., 2011). Based on the neurotoxicity of MTAs, these drugs also exhibit primary toxicity, since neuronal cells rarely divide in adults (Argyriou et al., 2014). In this study, UCDK9M3 did not demonstrate mitotic cell death, but FBZ induced a similar apoptotic effect and decreased viability. Therefore, FBZ treatment may have mitosis-independent toxicity in UCDK9M3 cells, and other cells may also share those effects.

In conclusion, FBZ treatment in canine melanoma cells was effective in inducing G2/M arrest and mitotic slippage, along with an apoptotic effect leading to mitotic catastrophe. Further in vivo studies are needed to determine potential clinical relevance of these findings.

ACKNOWLEDGEMENTS

This manuscript is written based on the master's thesis of author Sehoon Kim. We wish to thank to Dr. Takayuki Nakagawa, Department of Veterinary Surgery, the University of Tokyo for providing LMeC and KMeC cell lines. We also wish to thank Dr. Michael Kent from the Center for Companion Animal Health, University of California Davis School of Veterinary Medicine for supplying the UCDK9M3, UCDK9M4 and UCDK9M5 cell lines. This study publication was supported by 'Cooperative Research Program of Center for Companion Animal Research (Project No. PJ01404502): Rural Development Administration, Republic of Korea'.

CONFLICT OF INTEREST

There is no conflict of interest.

ETHICAL APPROVAL

The authors confirm that the ethical policies of the journal, as noted on the journal's author guidelines page, have been adhered to. No ethical approval was required as five canine melanoma cell lines had been previously published.

AUTHOR CONTRIBUTIONS

Sehoon Kim: conceptualisation; data curation; formal analysis; investigation; methodology; project administration; validation and visualisation; writing – original draft. Seo-In Choi: investigation. Robert B. Rebhun: resources, critical review.

DATA AVAILABILITY STATEMENT

Data openly available in a public repository that issues datasets with DOIs.

PEER REVIEW

The peer review history for this article is available at <https://publons.com/publon/10.1002/vms3.733>

ORCID

Sehoon Kim  <https://orcid.org/0000-0002-2616-6610>

Robert B. Rebhun  <https://orcid.org/0000-0002-8047-3494>

REFERENCES

- Aina, O. H., Maeda, Y., Harrison, M., Zwingerberger, A. L., Walker, N. J., Lam, K. S., & Kent, M. S. (2011). Canine malignant melanoma alpha-3 integrin binding peptides. *Veterinary Immunology and Immunopathology*, 143(1-2), 11-19. <https://doi.org/10.1016/j.vetimm.2011.05.018>
- Argyriou, A. A., Kyritsis, A. P., Makatsoris, T., & Kalofonos, H. P. (2014). Chemotherapy-induced peripheral neuropathy in adults: A comprehensive update of the literature. *Cancer Management and Research*, 6(1), 135-147. <https://doi.org/10.2147/CMAR.S44261>
- Blagosklonny, M. V. (2007). Mitotic arrest and cell fate: Why and how mitotic inhibition of transcription drives mutually exclusive events. *Cell Cycle*, 6(1), 70-74. <https://doi.org/10.4161/cc.6.1.3682>
- Bolon, B., Calderwood Mays, M. B., & Hall, B. J. (1990). Characteristics of canine melanomas and comparison of histology and DNA ploidy to their biologic behavior. *Veterinary Pathology*, 27(2), 96-102. <https://doi.org/10.1177/030098589002700204>
- Castedo, M., Perfettini, J. L., Roumier, T., Andreau, K., Medema, R., & Kroemer, G. (2004). Cell death by mitotic catastrophe: A molecular definition. *Oncogene*, 23(16 REV. ISS. 2), 2825-2837. <https://doi.org/10.1038/sj.onc.1207528>
- Cheng, B., & Crasta, K. (2017). Consequences of mitotic slippage for antimicrotubule drug therapy. *Endocrine-Related Cancer*, 24(9), T97-T106. <https://doi.org/10.1530/ERC-17-0147>
- DiPaola, R. S. (2002). To arrest or not to G2-M cell-cycle arrest. *Clinical Cancer Research*, 8(November), 3311-3314.
- Dogra, N., Kumar, A., & Mukhopadhyay, T. (2018). Fenbendazole acts as a moderate microtubule destabilizing agent and causes cancer cell death by modulating multiple cellular pathways. *Scientific Reports*, 8(1), 1-15. <https://doi.org/10.1038/s41598-018-30158-6>
- Doudican, N., Rodriguez, A., Osman, I., & Orlow, S. J. (2008). Mebendazole induces apoptosis via Bcl-2 inactivation in chemoresistant melanoma cells. *Molecular Cancer Research*, 6(8), 1308-1315. <https://doi.org/10.1158/1541-7786.MCR-07-2159>
- Endo, Y., Saeki, K., Watanabe, M., Miyajima-Magara, N., Igarashi, M., Mochizuki, M., Nishimura, R., Sugano, S., Sasaki, N., & Nakagawa, T. (2020). Spindle assembly checkpoint competence in aneuploid canine malignant melanoma cell lines. *Tissue & Cell*, 67, 101403. <https://doi.org/10.1016/j.tice.2020.101403>
- Galluzzi, L., Vitale, I., Aaronson, S. A., Abrams, J. M., Adam, D., Agostinis, P., Alnemri, E. S., Altucci, L., Amelio, I., Andrews, D. W., Annicchiarico-Petruzzelli, M., Antonov, A. V., Arama, E., Baehrecke, E. H., Barlev, N. A., Bazan, N. G., Bernassola, F., Bertrand, M., Bianchi, K., Blagosklonny, M. V., ... Kroemer, G. (2018). Molecular mechanisms of cell death: Recommendations of the Nomenclature Committee on Cell Death 2018. *Cell Death & Differentiation*, 25(3), 486-541. <https://doi.org/10.1038/s41418-017-0012-4>
- Gao, P., Dang, C. V., & Watson, J. (2008). Unexpected antitumorigenic effect of fenbendazole when combined with supplementary vitamins. *The Journal of the American Association for Laboratory Animal Science*, 47(6), 37-40.
- Inoue, K., Ohashi, E., Kadosawa, T., Hong, S. H., Matsunaga, S., Mochizuki, M., Nishimura, R., & Sasaki, N. (2004). Establishment and characterization of four canine melanoma cell lines. *The Journal of Veterinary Medical Science*, 66(11), 1437-1440. <https://doi.org/10.1292/jvms.66.1437>
- Jordan, M., & Kamath, K. (2007). How do microtubule-targeted drugs work? An overview. *Current Cancer Drug Targets*, 7(8), 730-742. <https://doi.org/10.2174/156800907783220417>
- Kisurina-Evgen'eva, O. P., Briantseva, S. A., Stil', A. A., & Onishchenko, G. E. (2006). Antimicrotubule agents can activate different apoptotic pathways. *Biofizika*, 51(5), 875-879.
- Koch, G. (2017). Tubulin inhibitors targeting the colchicine binding site: A perspective of privileged structures. *Chimia (Aarau)*, 71(10), 643. <https://doi.org/10.2307/j.ctvncw0d0.18>
- Komlodi-Pasztor, E., Sackett, D., Wilkerson, J., & Fojo, T. (2011). Mitosis is not a key target of microtubule agents in patient tumors. *Nature Reviews Clinical Oncology*, 8(4), 244-250. <https://doi.org/10.1038/nrclinonc.2010.228>
- Lai, S. R., Castello, S. A., Robinson, A. C., & Koehler, J. W. (2017). In vitro anti-tubulin effects of mebendazole and fenbendazole on canine glioma cells. *Veterinary and Comparative Oncology*, 15(4), 1445-1454. <https://doi.org/10.1111/vco.12288>
- Lara-Gonzalez, P., Westhorpe, F. G., & Taylor, S. S. (2012). The spindle assembly checkpoint. *Current Biology*, 22(22), R966-R980. <https://doi.org/10.1016/j.cub.2012.10.006>
- Li, L., Jiang, S., Li, X., Liu, Y., Su, J., & Chen, J. (2018). Recent advances in trimethoxyphenyl (TMP) based tubulin inhibitors targeting the colchicine binding site. *European Journal of Medicinal Chemistry*, 151, 482-494. <https://doi.org/10.1016/j.ejmech.2018.04.011>
- Mc Gee, M. M. (2015). Targeting the mitotic catastrophe signaling pathway in cancer. *Mediators of Inflammation*, 2015. <https://doi.org/10.1155/2015/146282>
- McKellar, Q. A., Galbraith, E. A., & Baxter, P. (1993). Oral absorption and bioavailability of fenbendazole in the dog and the effect of concurrent ingestion of food. *Journal of Veterinary Pharmacology and Therapeutics*, 16(2), 189-198. <https://doi.org/10.1111/j.1365-2885.1993.tb00163.x>
- McKellar, Q. A., Harrison, P., Galbraith, E. A., & Inglis, H. (1990). Pharmacokinetics of fenbendazole in dogs. *Journal of Veterinary Pharmacology and Therapeutics*, 13(4), 386-392. <https://doi.org/10.1111/j.1365-2885.1990.tb00793.x>
- Obradovich, D. (2016). *Small animal clinical oncology*. CRC Press. <https://doi.org/10.1201/9781315381855>
- Pinto, L. C., Mesquita, F. P., Soares, B. M., Soares, B. M., da Silva, E. L., Puty, B., de Oliveira, E., Burbano, R. R., & Montenegro, R. C. (2019). Mebendazole induces apoptosis via C-MYC inactivation in malignant ascites cell line (AGP01). *Toxicology In Vitro*, 60(May), 305-312. <https://doi.org/10.1016/j.tiv.2019.06.010>
- Portugal, J., Mansilla, S., & Bataller, M. (2009). Mechanisms of drug-induced mitotic catastrophe in cancer cells. *Current Pharmaceutical Design*, 16(1), 69-78. <https://doi.org/10.2174/138161210789941801>
- Rieder, C. L., & Maiato, H. (2004). Stuck in division or passing through: What happens when cells cannot satisfy the spindle assembly

- checkpoint. *Developmental Cell*, 7(5), 637-651. <https://doi.org/10.1016/j.devcel.2004.09.002>
- Rogers, R. S. (2000). Malignant melanoma in the 21st century. *International Journal of Dermatology*, 39(3), 178-179. <https://doi.org/10.1046/j.1365-4362.2000.00875.x>
- Sasaki, J. I., Ramesh, R., Chada, S., Gomyo, Y., Roth, J. A., & Mukhopadhyay, T. (2002). The anthelmintic drug mebendazole induces mitotic arrest and apoptosis by depolymerizing tubulin in non-small cell lung cancer cells. *Molecular Cancer Therapeutics*, 1(13), 1201-1209.
- Schmit, J. (2013). In vitro anti-cancer effects of benzimidazoles on the canine osteosarcoma D17 cell line. MS thesis. <http://hdl.handle.net/2142/45401>
- Shi, J., Zhou, Y., Huang, H. C., & Mitchison, T. J. (2011). Navitoclax (ABT-263) accelerates apoptosis during drug-induced mitotic arrest by antagonizing Bcl-xL. *Cancer Research*, 71(13), 4518-4526. <https://doi.org/10.1158/0008-5472.CAN-10-4336>
- Singh, R., George, J., & Shukla, Y. (2012). Retraction: Role of senescence and mitotic catastrophe in cancer therapy. *Cell Division*, 7, 1-12. <https://doi.org/10.1186/1747-1028-7-15>
- Stanton, R. A., Gernert, K. M., Nettles, J. H., & Aneja, R. (2011). Drugs that target dynamic microtubules: A new molecular perspective. *Medicinal Research Reviews*, 31(3), 443-481. <https://doi.org/10.1002/med.20242>
- Vail, D. M. (2020). *Withrow and MacEwen's small animal clinical oncology* (6th edn.). Elsevier Inc.
- Vitale, I., Galluzzi, L., Castedo, M., & Kroemer, G. (2011). Mitotic catastrophe: A mechanism for avoiding genomic instability. *Nature Reviews Molecular Cell Biology*, 12(6), 385-392. <https://doi.org/10.1038/nrm3115>
- Zhu, Y., Zhou, Y., & Shi, J. (2014). Post-slippage multinucleation renders cytotoxic variation in anti-mitotic drugs that target the microtubules or mitotic spindle. *Cell Cycle*, 13(11), 1756-1764. <https://doi.org/10.4161/cc.28672>

How to cite this article: Kim, S., Perera, S. K., Choi, S.-I., Rebhun, R. B., & Seo, K. W. (2022). G2/M arrest and mitotic slippage induced by fenbendazole in canine melanoma cells. *Veterinary Medicine and Science*, 8, 966-981. <https://doi.org/10.1002/vms3.733>